Measurement of Large Scale Oil Spill Burns

D. Evans, W. Walton, H. Baum, R. Lawson, R. Rehm, R. Harris
National Institute of Standards and Technology
Gaithersburg, Maryland

A. Ghoniem
Massachusetts Institute of Technology
Cambridge, Massachusetts

J. Holland
Consultant
Wheaton, Maryland

ABSTRACT

Research has shown that burning can be an effective means to remove oil from the surface of the water. The combustion characteristics of crude oil have been measured in large laboratory tests using a nominal one meter diameter pool fire. This work reports on progress mid-way through a 2½ year research program. The objective of this research is to develop measurement equipment and calculations that can be used to characterize oil spill burning at operational scale during field trials of the technology. Field scale measurement techniques for fire radiation, smoke yield, particulate sampling, plume trajectory are described. Progress in the calculation of particulate deposition downwind of the burn site is presented.

INTRODUCTION

Response to oil spills includes considerations of oil containment, recovery, disposal and the logistics of delivering adequate response equipment quickly to the spill site. Particularly in remote areas, the use of burning as a oil spill response method is attractive. Burning requires a minimum of equipment, and because the oil is gasified during combustion, the need for physical collection, storage, and transport of recovered product is reduced to the few percent of the original spill volume that remains as residue after burning. The technology of oil spill burning and other response methods have been reviewed recently [1, 2, 3].

The technology of greatest interest is that designed to burn oil in-place. Present work is directed at burning spills under natural confinement such as within ice leads or with artificial confinement within fire-proof collection booms. Using the latter approach, approximately 15,000 gallons of oil from the recent Exxon Valdez spill were confined after nearly two days in the water and burned. The resulting fire lasting approximately 45 minutes consumed all but 300 gallons of residue that remained in the boom [4].

Environment Canada. Arctic and Marine Oil Spill Program Technical Seminar, 13th. June 6-8, 1990, Edmonton, Alberta, Canada, Environment Canada, Ottawa, Ontario, 1-38 pp, 1990.

Burning oil spills in-place normally produces a visible smoke plume containing soot and other combustion products produced in the burning. The smoke plume produced by burning of crude oil spills and the possibility of undesirable combustion products carried in the plume have led to public concerns over the effects of burning large crude oil spills. Lack of knowledge about heat and radiation from large fires has also hampered application of burning to oil spills because of unresolved questions of personnel and equipment safety.

Burning may be thought of as an emerging technology for response to oil spills. The National Institute of Standards and Technology (NIST) is the U.S. National laboratory with the mission to aid industry in the development of new methods to improve productivity. In the area of technology for oil spill response, this includes providing the means to answer public concerns about the consequences of burning to provide a basis for evaluation of its use by industry. Under funding from the Minerals Management Service, U.S. Department of the Interior, with contributions from the United States Coast Guard, U.S. Department of Transportation, and unique technical assistance from the Technology Development and Technical Services Branch of Environment Canada, NIST has carried on a program of oil spill burning research since 1985.

BACKGROUND

In the five year research program, specialized large laboratory scale fire facilities at NIST have been used to investigate the fire dynamics and chemistry of the oil spill burning process. These studies have provided new quantitative information about the crude oil burning process. For example, laboratory measurements [5] have shown that the soot yield, the mass fraction of oil converted to soot during burning, is nominally 10 percent based on tests with Alberta Sweet crude oil. Other technical results about burning rate and combustion products are contained in previous papers [5, 6, 7, 8].

As with any large natural or accidental event that may impact the environment, opportunities to observe and measure the effects of large fires during emergency conditions are rare. Furthermore, permits to conduct large scale experiments that simulate oil spill burns at the appropriate scale and the large amount of funding needed to perform measurements at field scale are difficult to obtain. At best only infrequent opportunities will be available. Anticipating the sparsity of large scale test data, advanced calculations of plume dynamics have been part of the NIST research program since the beginning. These calculations provide a means to extrapolate laboratory measurements of burning conditions and combustion products through predictions of visible plume trajectory and deposition of products downwind of postulated large oil spill burns. Simply, these methods under development in the NIST research program will provide a means to perform hundreds of calculational experiments to add to the available experience

from actual field tests. Examples of progress in the development of these calculation methods are contained in previous papers [5, 6, 7, 8].

The large accidental spill of crude oil from the tanker Exxon Valdez in Prince William Sound, Alaska focused national attention on oil spill response technology. In cooperation with a team of interested parties from industry and government planning has begun for operational tests of burning on an experimental oil spill at sea in 1991. In preparation for these tests, the NIST research program was expanded to develop means to measure the burning characteristic of these large fires. To accomplish this task, work was started to make laboratory methods and equipment used in previous studies at NIST robust enough for use in the field. In some cases, completely new measurement techniques were required because laboratory methods were inappropriate for field use or the measurements, such as plume trajectory, are only appropriate to large scale. This paper details the plans and progress to date in a 2½ year research program to move measurement of oil spill burning characteristics from the laboratory to the field using mid-scale 10 m to 15 m diameter fire tests to prove performance of the measurement equipment.

Mid-Scale Testing

As important to this research program as the eventual field tests, mid-scale tests will be performed to evaluate measurement techniques and provide personnel with the opportunity to gain working experience in the environment around large crude oil fires. As part of the interagency cooperation in this project, mid-scale tests are being planned for the summer of 1990 at the U.S. Coast Guard Fire and Safety Test Detachment located on Sand Island in Mobile Bay Alabama.

At this facility, oil pool fires up to 15 m in diameter can be burned in a tank welded to the deck of a 150 m surplus tanker which is used for fire testing. The tanker is moored in a lagoon of a 50 acre island in Mobile Bay, see Figure 1. As the ship is used routinely for fire testing, utilities and some measurement equipment are available on site.

MEASUREMENT PROGRAM

Fire Heat Release Rate (Burning Rate) History

Heat release rate is the primary burning characteristic of a fire. In the laboratory, oxygen consumption calorimetry [9] has been used to evaluate crude oil fire heat release rates [5, 6, 7,]. Estimations of heat release rate can be made also by multiplying the heat of combustion for a fuel times the mass loss rate. In the laboratory, mass loss rate can be determined easily by weighing the fuel.

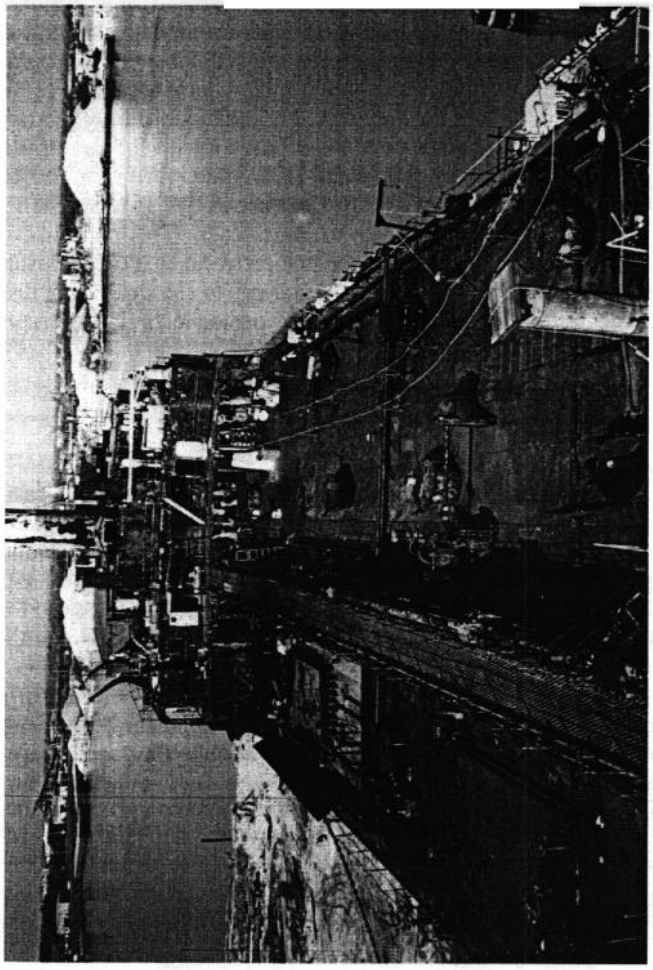

Figure 1 USCG fire test facility Mobile, Alabama.

In the field, there are no direct measurements for fire heat release rate. In a previous large scale oil burn test, [4] the average fuel consumption rate has been estimated by dividing the total mass of fuel consumed by the burning time. In that burn, 15,000 gallons of North Slope crude oil were consumed during 45 minutes of vigorous burning. The average fuel consumption rate during the vigorous burning was 330 gallons per minute. Thus, even in field burns the average burning rate is easily obtained if the amount of fuel consumed is known; and this average may be all that is needed when the fire is nominally constant in burning rate.

When the burning rate is not constant, more than an average rate is needed to characterize the combustion. It is possible that a technique can be developed for field use that uses measurements of surface thermal radiation, smoke plume trajectory, and burning area to calculate instantaneous fire heat release rate. Such a method will be developed and evaluated in mid-scale testing by correlating measurements of several fire diameters. Use of these correlations at field scale will be an extrapolation of the data beyond that correlated but within the same order of magnitude as the mid-scale tests.

Laboratory measurements of crude oil burning in pools up to 1.2 m in diameter have shown two distinct regions of burning, see Figure 2. After ignition there is a quiescent burning period with slightly decreasing heat release rate reflecting preferential depletion of high vapor pressure components from the fuel. The surface temperature of the burning oil maintains a temperature in the range of 250 to 350 °C. The hot oil below the burning surface eventually comes in contact with the water on which the oil is floating. In small scale tests with thick initial oil layers, the water boils, releasing vapor bubbles that burst at the surface and eject oil droplets into the flame. The increased flux of fuel causes the flame to flare up increasing the rate of heat release until extinction. In laboratory tests, Figure 2, the enhancement in burning rate by water boiling can be more than a factor of two. In large burns within booms being towed through the water [4] and large hydrocarbon pool fire tests conducted in Japan [10] enhanced burning due to water sublayer boiling has not been seen. There are two completely different mechanisms that could account for these observations.

In the case of oil burning while being moved over the water within a fire resistant confinement boom, ambient temperature water is continually being supplied below the oil layer. Thus, depending on the tow speed and current, the residence time for the burning oil over a given water mass may be insufficient to induce boiling. Figure 3 shows a schematic diagram of a laboratory apparatus built to measure oil burning characteristics under conditions simulating field conditions in which a contained burning oil mass is being moved on the water surface. For convenience, in this simulation the confined burning oil is kept stationary; and the water is flowed beneath it at selected speeds. Testing with this apparatus will provide insight into the effect of moving water layers on oil burning rate and residue remaining at flame extinction.

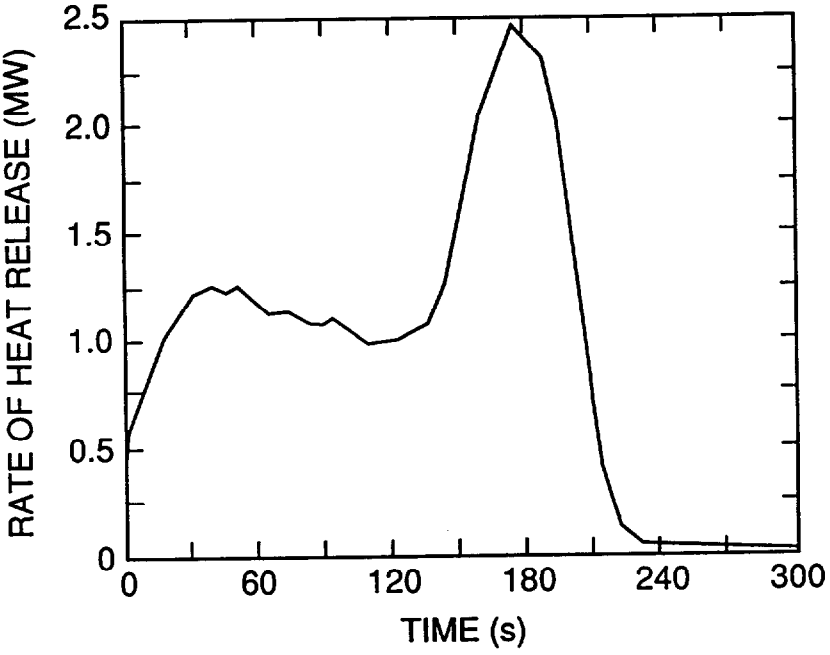

Figure 2 Measured heat release rate for 1.2 m diameter Alberta Sweet crude oil fire.

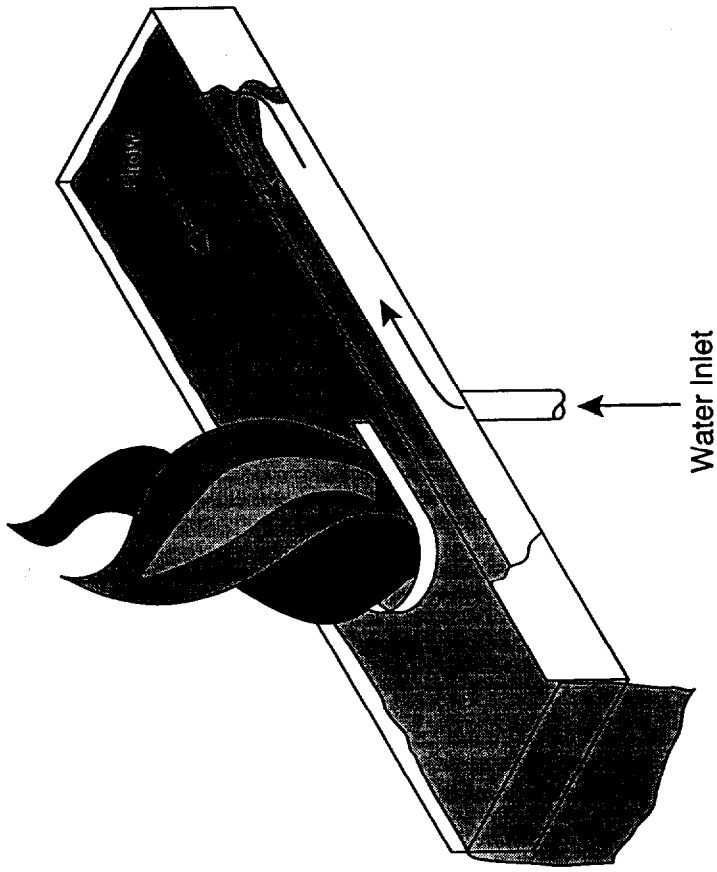

Figure 3 Schematic of boom simulation oil burning apparatus.

Maintaining a flow of cool water beneath the burning oil is only one factor in determining the conditions under which water sublayer boiling will occur during large scale burns in booms being towed through the water. Experiments in Japan at the Fire Research Institute have shown that there is an effect of scale as well. In their work for larger fires in which the fuel layer surface regression rate (or burning rate per unit area) was greater than that measured in smaller laboratory tests, no water sublayer boiling was seen. We postulate that in the larger pool fire tests conducted in Japan, up to 3 m in diameter, the onset of water sublayer boiling occurs when the burning oil layer is very thin. The onset of boiling for the larger scale fires may occur only for very thin layers representing the small depth that heat penetrates into the unburned fuel by thermal conduction from the hot surface because of increased fuel surface regression rate. The stirring of the shallow oil layer by boiling produces a sufficient temperature decrease to quench the burning. Therefore, in a large pool fire with increased burning rate per unit area as compared with small scale tests, the onset of water sublayer boiling produces flame extinction and not vigorous burning.

In field tests, both the large area and motion over the water of the burning oil will provide conditions unfavorable for water sublayer boiling. Mid-scale testing to be performed in this research program will provide greater insight into this effect.

Thermal Radiation

Measurements of thermal radiation from the burning oil are used to predict the potential hazard to personnel and equipment operating near the burn site. Thermal radiation measurements can also be used to predict the burning rate of the fuel. Correlations such as the ones developed by Shokri and Beyler [11] and Mudan and Croce [12] may be used to predict the radiative heat flux at a ground level target a given distance from the pool. These correlations are based primarily on gasoline, kerosene, JP-4 and JP-5 fires. Other large scale fire results which include data for crude oil have been reported by Koseki [10, 13]. Previous tests have shown the average surface emissive power of large sooty fires actually decreases with increasing diameter. This is probably a result of substantial radiation blocking by absorption in the thick black smoke carried around the flame by turbulent mixing. As a result, thermal radiation becomes a complex function of pool diameter. It remains to be seen whether this behavior can be quantified well enough to provide a measurement technique for the burning rate.

Thermal radiation to targets at various distances from the crude oil fires will be measured with Gardon type radiant heat flux gauges. These gauges are used routinely in fire safety research studies. The gauges measure the temperature difference between the center of a thin blackened surface and a thermal sink temperature at the edge. The radiant heat flux to the blackened surface is a function of the temperature difference.

Smoke Sampling

The sampling of smoke for chemical and yield analysis is a relatively easy task in the laboratory. This process consists of using an appropriate filter media such as PTFE with an 0.8 μm pore size for collecting the smoke particulates, a pump for drawing the smoke into the filter, and a constant flow rate controller. The mass of soot is determined by weighing the filter, and the filtered material is analyzed. In the laboratory, the equipment used for sampling can be of any reasonable size and weight, and is usually conveniently located on a test bench near the experiment. However, in the field with large fires, where the appropriate sample point in a smoke cloud may be several hundred feet in the air, this task of sampling becomes quite complex. With the need to sample well above ground level, the size and weight of an experimental package becomes critical. The efficiency of this experimental package takes on additional importance since sampling will be done in a constantly varying environment driven by the local weather conditions. Figure 4 shows the sampling system currently being used in this project. The largest part of this system is the sampling pump which is 15.7 cm long, 4.5 cm in diameter, and weighs 0.79 kg. This lightweight pump is identical to that flown as part of experiments on NASA Space Shuttle missions within the last year. The pump is operated from a simple 12 volt DC battery or power supply, and draws a constant flow rate of 10 liters per minute through a clean 47 mm filter. The filter holder is made of aluminum and is 5.5 cm long, 5.5 cm in diameter and weighs 0.16 kg. Clear plastic tubing is used to connect the system components. Filter media taken from this system during field tests will be returned to the laboratory so that PAH's and other important constituents may be measured.

Soot Production (Soot Yield)

Determinations of mass of soot produced per unit mass of fuel consumed has been done in laboratory tests using two methods [5]: stack particle flux sampling and the carbon balance method. Stack particle flux sampling is based on comparison of the mass of particulates collected from a known portion of the total smoke plume flow from the fire to the measured mass loss of the burning fuel during the same period of time. The carbon balance method determines the soot yield based on ratio of soot mass to the total mass of carbon found (soot plus mass of carbon contained in CO_2 and CO gases) in a sample of smoke plume combustion products. Of these two, only the carbon balance method is feasible for application to large fires.

A third method being investigated is isotopic tagging and tracing of particles by mass spectrometry [14]. This method also has the potential to measure soot deposition far downwind of a smoke source and therefore could be appropriate for use in the planned field tests.

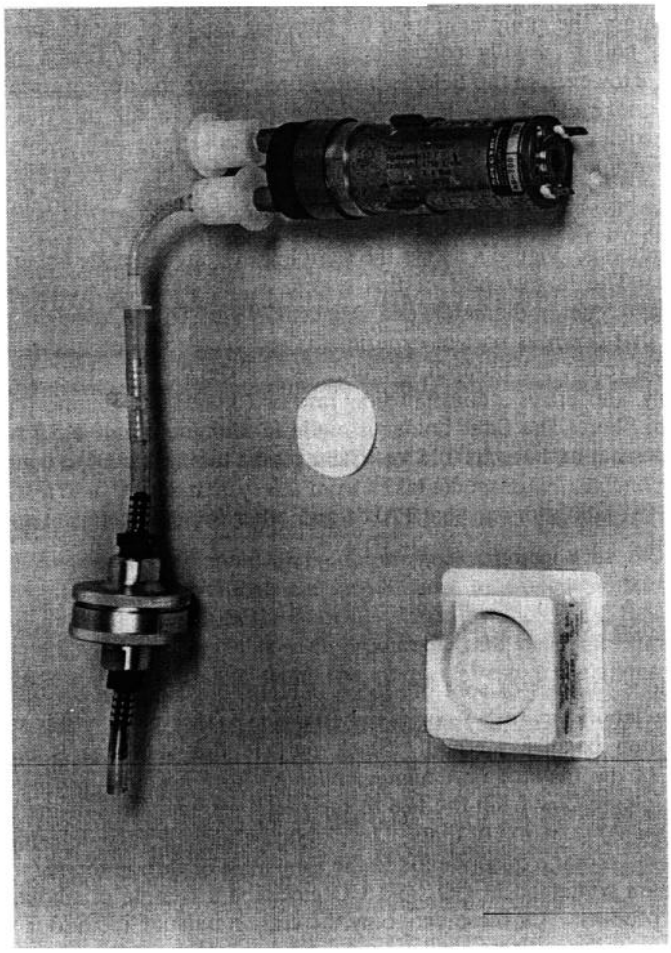

Figure 4 Pump and filter apparatus for smoke sampling.

The isotopic tagging technique involves addition of enriched isotopes of rare-earth elements into the fuel before combustion, and then measuring the perturbations in the natural isotopic ratios in aerosol particles collected downwind. In large scale oil burn tests being planned, particles collected downwind could be identified positively as originating from the oil spill burn and not other sources such as from ship engines. The isotopes used are nontoxic, chemically stable, nonradioactive, and relatively inexpensive, and can be detected with an ultimate sensitivity below 1 part in 10^{15} (mass/mass basis). This rivals or exceeds the sensitivity of the most sensitive inert tracer gases used to study the long-range transport of air masses and represents a more than 40,000-fold reduction in the amount of tracer material needed over previously-used tracer materials.

Since the tracer is added directly to the fuel before burning it is important to know if the tracer is liberated from the fuel during combustion proportionally with the crude oil consumed. Laboratory tests with the 0.6 m diameter pool fire and collection hood and soot sampling instrumentation used in previous studies [5] will be used to evaluate the liberation of the tracer into the combustion products during burning and determine the feasibility of the method for measurement of soot yield from crude oil burns. During these tests soot yield will be determined also by the stack particle flux sampling, a method developed by Mulholland, et al. [15] used in previous testing [5], for comparison with results from the new isotopic method. In these tests only 8 mg of enriched ^{150}Sm will be needed to treat 4 kg of oil needed in the test, a concentration of one part in 500,000. After collection the amount of tracer in the smoke particles will be determined by Inductive-Coupled Plasma Mass Spectrometry (ICP-MS) [14].

Smoke Concentration Measurements by Light Scattering

In order to measure the concentration of smoke in the fire plume rapidly and at many positions a small, light weight light scattering apparatus is being evaluated. The apparatus is shown in Figure 5. It uses a pulsed near-infrared light emitting diode source, a silicon detector, and collimating and filtering optics to sense the light scattered over a forward angle of 45 to 95 degrees by airborne particles passing through a open sensing volume. The airborne particles pass through the sensing chamber as a result of natural air currents. The device can accurately measure concentrations over a range of 0.01 to 100 mg/m^3 with a particle size range up to 10 μm. This instrument measures 10 x 10 x 5 cm and weighs 0.45 kg and is operated by a self-contained rechargeable battery. The meter has an analog output which is connected to a miniature data logger also shown in figure 5 to record measurements during flight. The combined weight of the meter and data logger is 1.05 kg. This meter system will be used at various known locations in the smoke plume with the mid-scale and large scale fire experiments. It is intended for measurement of smoke concentration along the near field plume trajectory.

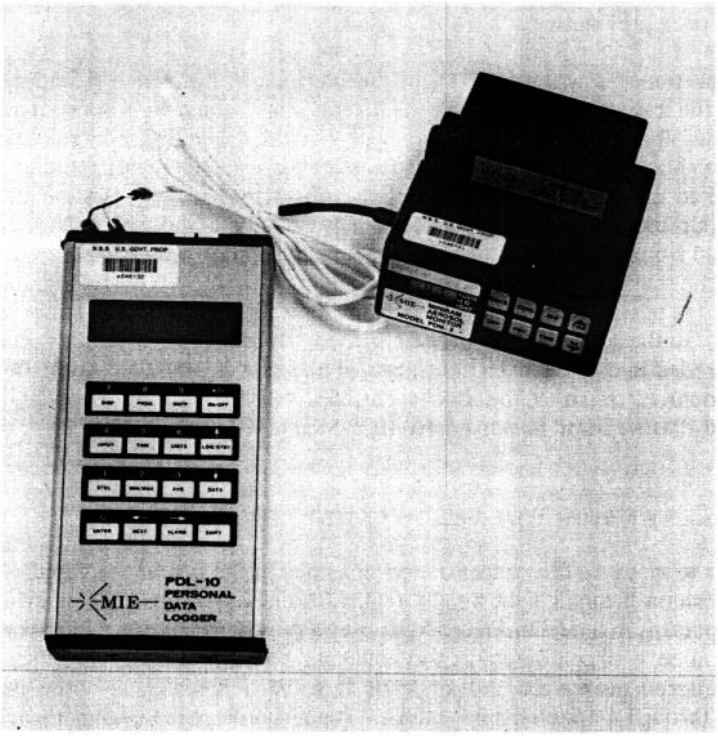

Figure 5 Light scattering apparatus for smoke concentration measurements.

Calibration Experiment

A series of calibration tests were conducted to evaluate smoke concentration measurements made with the light scattering apparatus described in the previous section. Louisiana and North Slope crude oils were used as test materials. The tests were conducted using the ASTM, E662 Smoke Density Chamber (Figure 6) so that the filter samples and the light scattering apparatus results could be evaluated and correlated with standardized optical density (OD) measurements made with the chamber. In addition, reduced data from the tests could be used to compare optical properties of smoke from crude oil with those from other combustibles. All tests were performed without supplemental radiant heating available from electric heating coils in the Smoke Density Chamber. The oils were burned in small crucibles positioned in the chamber at a point where the smoke plume had a clear path to chamber's ceiling. This was done to minimize soot particle deposition on hardware exposed directly to the smoke plume.

Results from the smoke chamber tests showed that smoke concentration measured with the scattering apparatus agreed within 6 percent with concentrations measured by filter collection and weighing, over the range of 55 to 92 mg/m^3. The scattering apparatus as supplied from the manufacturer has a useful measurement range from 0.01 to 100 mg/m^3. By decreasing the sensitivity of the apparatus broader measurement ranges are available. Mid-scale tests together with smoke plume calculations will provide information needed to select the sensitivity range of the scattering apparatus for the field scale tests.

Comparisons of optical density per meter as a function of mass concentration in air of the smoke from the crude oil fires to those of other combustibles are shown in Figure 7. Optical density is a logarithmic measure of light transmittance equal to $\log_{10} (I_0/I)$, where I_0 is the light intensity transmitted without obscuration and I is that for the obscuring sample. The data from both the Louisiana and North Slope crude oils are consistent with the correlation of data generated on a wide range of organic materials tested by King [16] and reported by Seader and Ou [17]. Thus smoke produced from burning crude oil is similar in optical characteristics to other common materials.

INSTRUMENT TRANSPORT AND POSITIONING

In both the mid-scale and field scale crude oil burn tests, measurements are to be made in the smoke plume emitted from the fire. Various means of positioning instruments within the smoke plume have been evaluated. These included: towers, manned aircraft, fixed winged and helicopter remotely piloted aircraft, and balloons or mini-blimps.

In the mid-scale tests, as much instrumentation as possible will be evaluated so that measurement methods of various levels of accuracy and performance may be

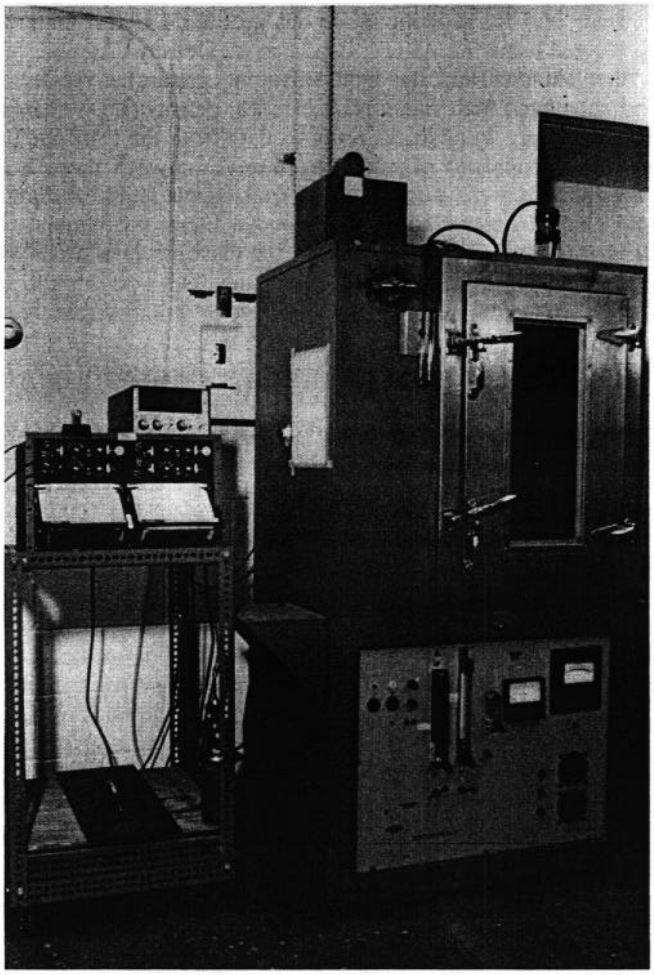

Figure 6 ASTM E662 Smoke Density Chamber.

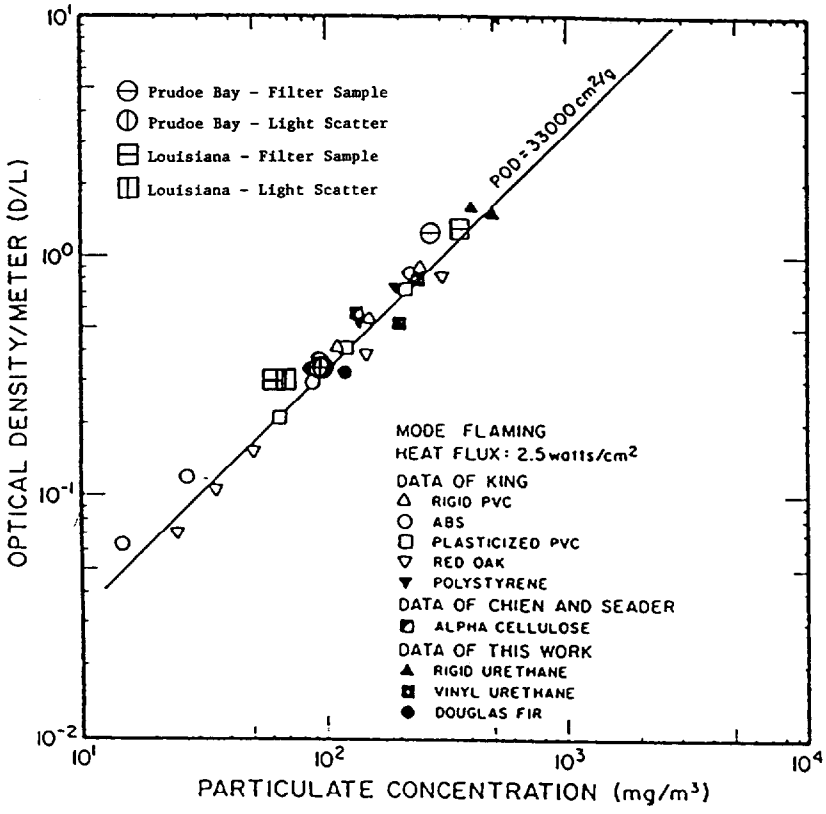

Figure 7 Optical Density versus smoke concentration for crude oils and other materials.

compared. This includes methods used in previous NIST laboratory tests and other field instruments in environmental air sampling.

Towers

Towers of useful height for fire plume measurements must be fixed or guyed for stability. The lack of mobility limits the usefulness of towers for plume measurements except for the area close to the source. Towers are projected for use in the mid-scale tests for mounting instruments near the edge of the crude oil pool and for supporting thermocouple arrays to obtain temperature measurements directly above the burning fuel.

Fixed-wing and Helicopter Remotely Piloted Aircraft

Two remotely piloted aircraft were evaluated for carrying instrument packages and providing video images during the mid-scale and field scales tests. A small light weight plane (Figure 8), developed for military surveillance, carries a black and white television camera and transmitting the video signal to a ground station for recording. The on-board camera is also used by the "pilot" on the ground to fly the craft by viewing a camera monitor. Even though the small aircraft could provide video images from above the fire, this type of support should be available with manned aircraft.

The capabilities of a larger aircraft (Figure 9) that carried a color camera and has capability to transport a 12 kg instrument package with a range of 25 km were examined. This aircraft was judged to be too difficult to launch and recover during the type of testing planned for this project. Also, the flight speed of the plane would severely limit the sampling time at any position. Finally, the large aircraft requires extensive training for the operator to become proficient with the controls for the craft.

A helicopter of the type used routinely by Environment Canada can be used for making measurements during both the mid-scale and field scale tests. This craft (Figure 10) is capable of carrying a video camera and a 9 kg instrument package and can hover at locations to collect samples. As with the large fixed-wing aircraft, operation of the small helicopter requires extensive training. It is planned to use this type of helicopter to gather data on smoke concentration at various positions within the smoke plume from the crude oil fires.

Balloons and Mini-Blimps

A tethered mini-blimp is being evaluated as the primary means of positioning instrumentation for soot collection in the smoke plume. Preliminary control and

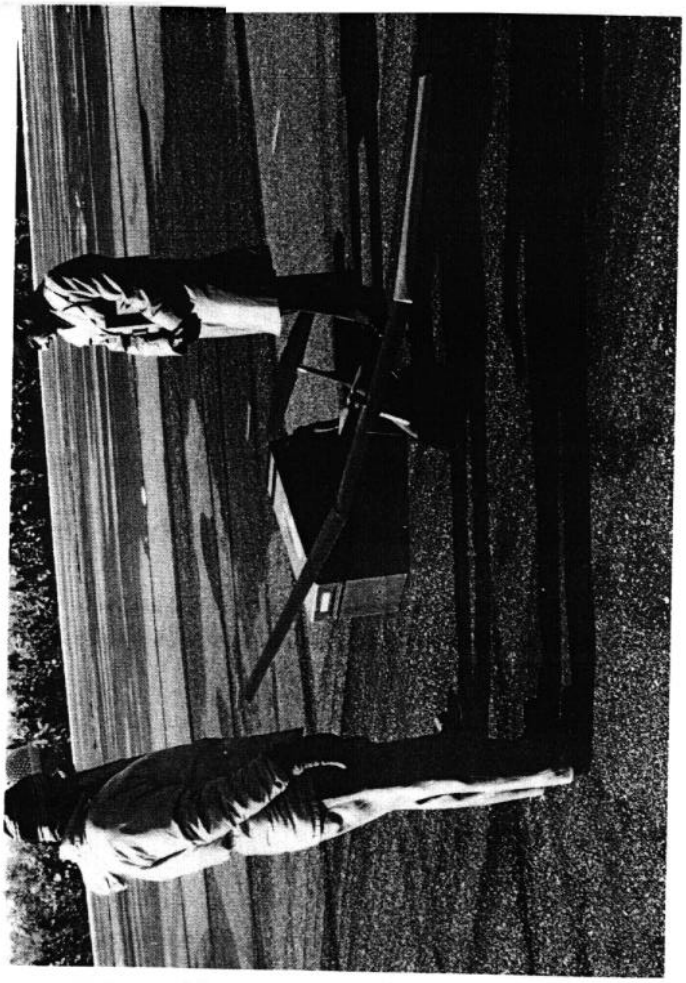

Figure 8 Small remote control aircraft.

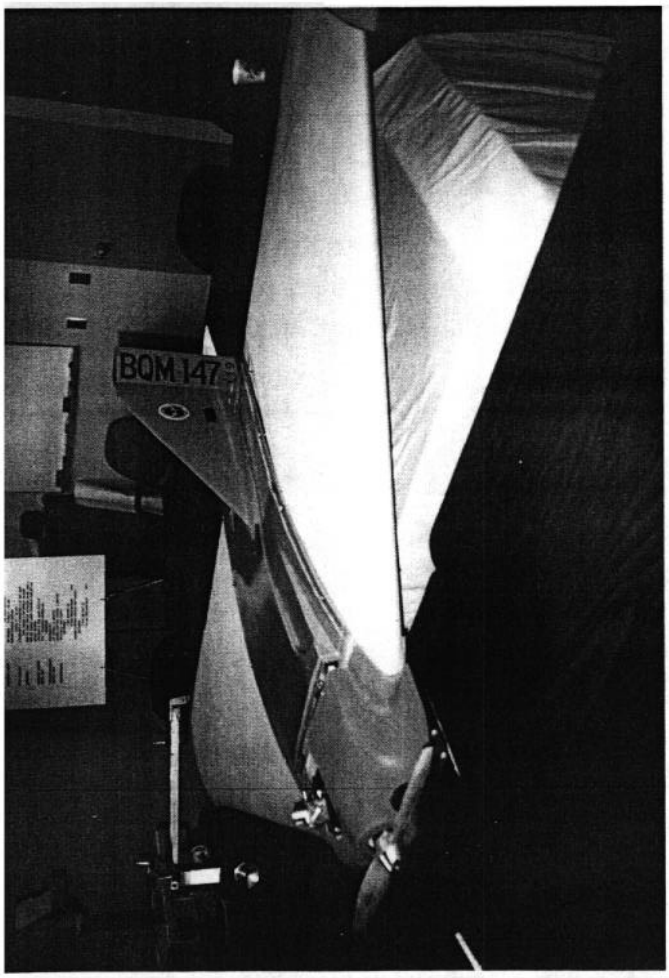

Figure 9 Large remote control aircraft.

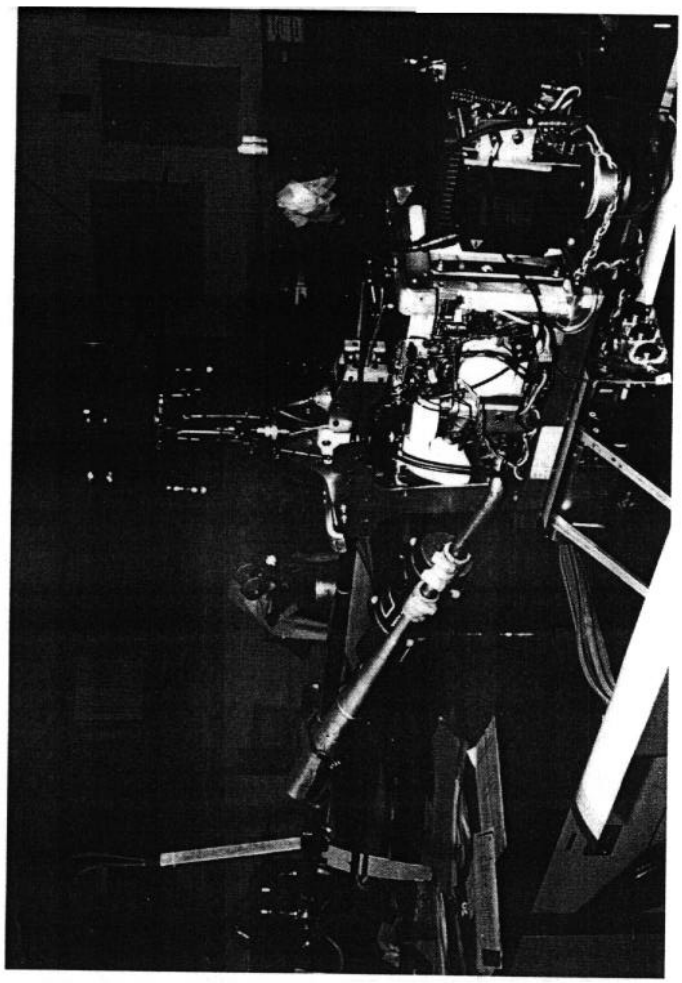

Figure 10 Environment Canada remote control helicopter.

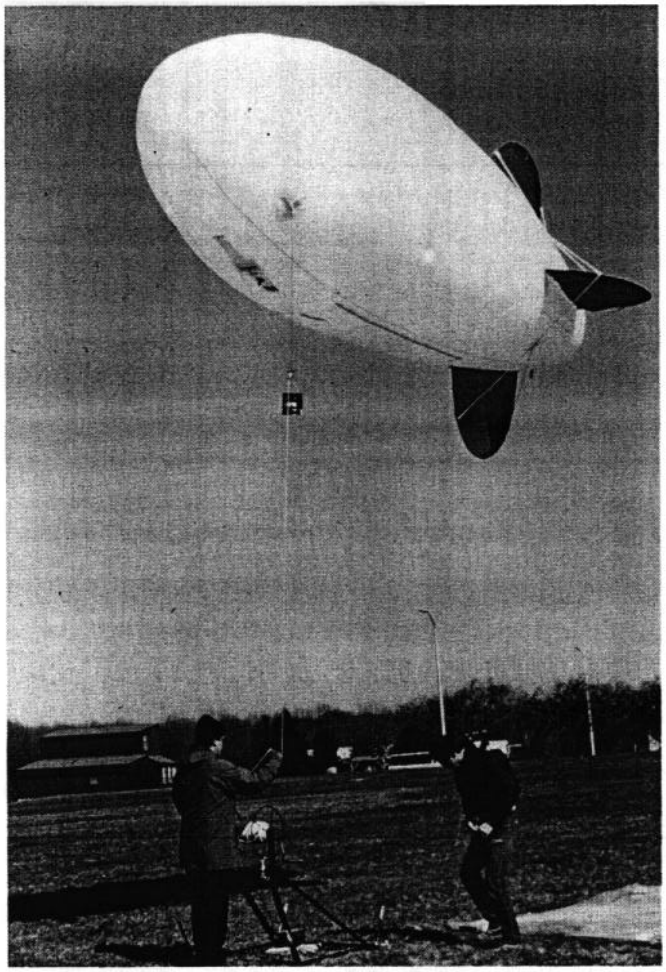

Figure 11 Mini-blimp.

instrument payload tests have been carried out to evaluate operational limits of the blimp, Figure 11. The blimp can carry a 4 kg instrument package to several hundred feet above ground level. It can be readily be moved from one location to another. Launch and recovery procedures are simple, and little time is needed to learn how to safely maneuver the blimp. Mini-blimps will be used in the mid-scale tests for positioning instrumentation packages. Experience in these tests will determine if the system is practical for the field scale tests.

Weather Station

In order to perform calculations on plume dispersion, data on local atmospheric conditions is needed. To measure these condition at the burn site two different types of weather stations have been acquired. One station provides a profile of conditions from the ground to 150 m altitude by transporting it on a tethered weather balloon. This instrument provides information on wind speed, direction, temperature and barometric pressure. At both the mid-scale and field scale tests this weather station will be deployed upwind of the burn site to measure atmospheric profiles prior to tests and continuously at one elevation during the test.

At both the mid-scale and field scale tests, a ground weather station will be deployed just up-wind of the test site. It will provide continuous weather information during the burn. The ground based station provides the same weather data as received from the station aloft.

SMOKE PLUME TRAJECTORY AND PARTICLE SETTLING MODELS

Observations During Mid-Scale Fire Tests

Mid-scale testing is a critical part of the measurement program in this project. In November, the research staff was given the opportunity to attend 15 m diameter pool fire burns of diesel fuel at the Farrier Firefighting Facility at Norfolk, Virginia. These large scale fires provided valuable experience that will be used in the design of practical instrumentation packages and safety plans for future crude oil burns. Observation from the tests are generally instructive and provide a specific case for comparison of classical predictive methods for smoke plume dispersion.

On the day of the tests the wind speed was approximately 3 m/s which is considered near the upper limit for effective measurement in mid-scale tests. This wind has a strong effect on the fire plume down to the base of the 15 m diameter fire (Figure 12a). The smoke moved generally upward and then turned sharply downwind (Figure 12b). The thermal radiation from the fires was such that one

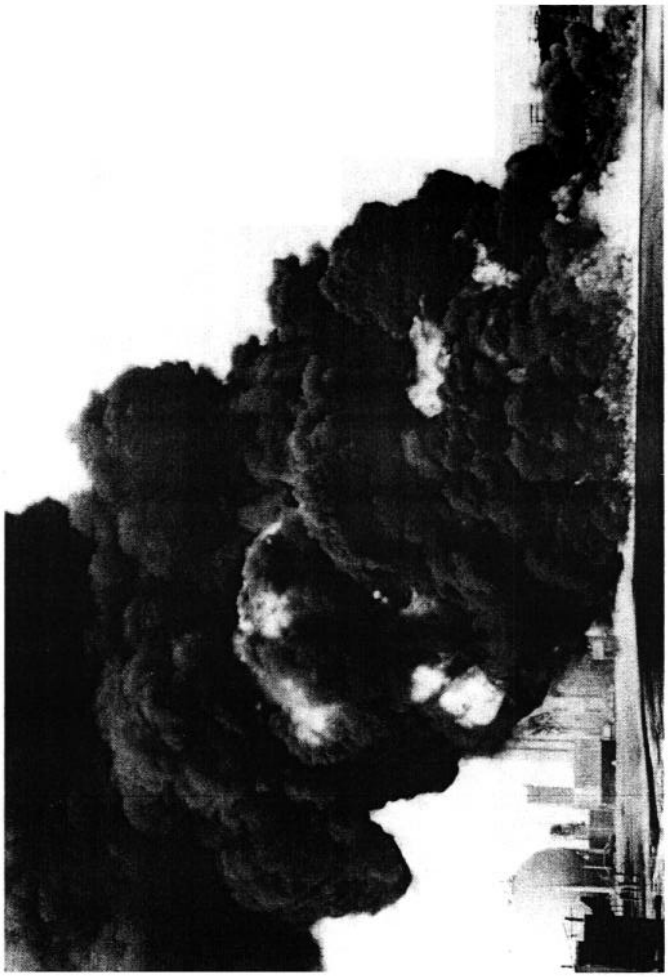

Figure 12a Mid-scale 15 m diameter diesel fuel fire during the first 30 seconds after ignition.

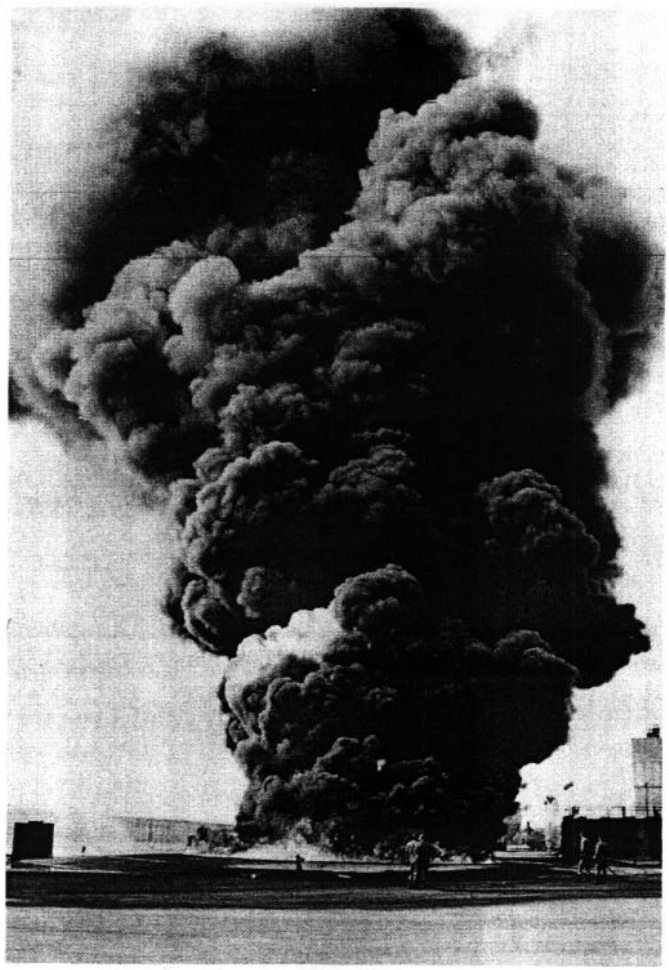

Figure 12b Smoke plume rises and turns downwind during peak burning period.

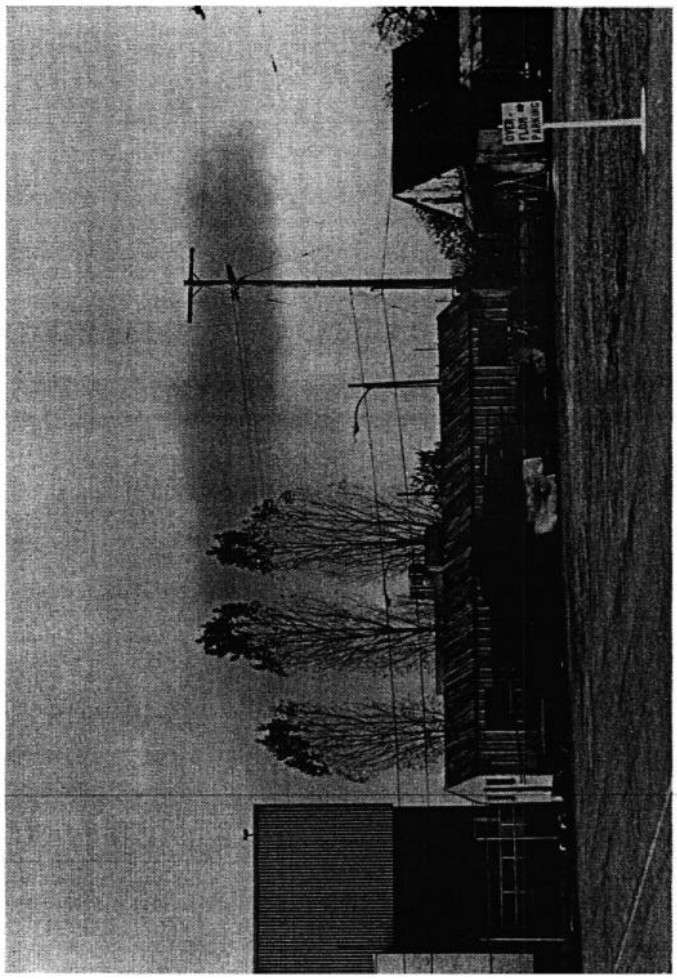

Figure 12*c* Smoke layer visible downwind 1/2 hour after test.

could easily approach to within approximately 1 to 2 fire diameters without feeling pain on bare skin. Most of the flame was obscured by the smoke. The smoke in the plume directly above the fires was sufficient to obscure the sun. As the smoke traveled away from the fire, it appeared to reach a constant stratification. The smoke was still visible downwind as a well defined cloud nearly a half-hour after the tests were terminated (Figure 12c).

Classical Analysis

Since the mid-1960s plume rise and dispersion from stacks has been an active area of research because of environmental concern about the dispersion of stack gases from manufacturing and power generation facilities [18]. To some extent this technology can be generalized to the dispersion of products from large diameter fires. For one of the 15 m diameter diesel fuel at the Farrier Firefighting Facility at Norfolk Virginia, an analysis of plume rise height, width, and depth as a function of distance from the burn was performed using classical correlations for plume dispersion. The predictions were compared with the video record of the test. The results given below indicate the sensitivity of plume rise height predictions to different assumed atmospheric conditions.

The plume height formulas given by Briggs [18] were used as the basis for the analysis. They are:

$$z_c = 1.6\, F_b^{1/3}\, x^{2/3}\, u^{-1} \qquad (1)$$

for the period before atmospheric stability begins to limit plume rise, for example within a neutrally stable mixed layer, and

$$z_c = 2.6 \left(\frac{F_b}{u\, s}\right)^{1/3} \qquad (2)$$

for the stabilization level in a stably stratified atmosphere, where

z_c is the height of the center of the cloud;

$F_b = g\, V_o\, (T_o - T_a)/T_o$, with

g = acceleration of gravity = 9.8 ms^{-2},

V_o = volume flux at the source = $\pi\, r_o^2 w_o$,

r_o = radius of plume at the level z_o, r_o taken as 7.5 m,

z_o = is a level where all heat has been added, z_o taken as 7.5 m,

w_o = vertical velocity at z_o,

T_a = ambient temperature, taken as 286 K,

T_o = average plume temperature at z_o,

x = distance downwind,

u = mean wind speed, taken as 4 ms^{-1},

$s = g(\partial T_a/\partial Z + \Gamma)/T_a$,

Γ = adiabatic lapse rate = 0.01 Km^{-1}

Determination of many of the values needed in these correlations depended on careful and detailed analysis of the video tape record of the test. At future mid-scale tests efforts will be made to measure as many as possible, but even analysis of near fire plume parameters and plume trajectory will always depend on analysis of video records. Parameters for this calculation were evaluated as follows.

To evaluate w_o and T_o a number of sequences of frames of the fires were examined and measurements were made of the coordinates of traceable features of the close-in smoke plume where the width of the pool (15 m) could be used as a scale reference. Two sets of smoke cloud element trajectories were analyzed. During period 1, about 40 seconds in duration immediately after fuel ignition, the fire had not reached full intensity. After 2.5 minutes of burning the fire reached peak intensity. During this period flames were visible up to at least 20 m height. Shortly thereafter the fire was extinguished by hose streams.

Smoothed coordinates (x,z) of cloud elements were calculated by 4-point running means for trajectories on which readings had been taken at intervals of 0.2 s, or 5-point running means for those with intervals less than 0.2 s. Horizontal (u) and vertical (w) velocity components were calculated from the least-squares linear trend in x and z over these same 4- or 5-point data samples. In this way 185 sets of x,z,u and w were obtained.

As parcel trajectories at levels below 7.5 m were significantly influenced by addition of heat, values were estimated for w_o based on the video data samples above 7.5 m. These were 2.0 m/s for period 1 and 3.5 m/s for period 2. A typical effective flame temperature of 900 K was assumed to be the average at this level for period 2 ("mid-burn") while a more moderate 600 K was assumed for period 1 ("early burn"). These vertical velocities and temperatures are compatible with plume heating rates of the order of 1 and 0.5 MW/m^2 respectively.

The measured average value of u, 2.5 m/s perpendicular to the line of camera sight, for the trajectories above 7.5 m, implies a total speed of 3.5 m/s. This is consistent with the assumed ambient wind speed of 4 m/s based on recorded measurements at nearby weather stations, considering that the horizontal motion of the rising plume may not have been in equilibrium with the horizontal wind at that level.

Values for the stability parameter, s, were inferred from weather observations. Prior to the burn the sky was broken to overcast and as the tests were conducted near the end of November, the solar attitude, even at noon, was only 35° [19]. The wind was coming off the ocean with only a short fetch over land. The ocean and bay temperatures typically are slightly lower than the observed air temperatures,which showed very small diurnal increases of 1 to 3 °C from 10 a.m. to noon, the approximate time of the burn. Upper air soundings recorded by the nearest weather station were nearly isothermal conditions in the lowest kilometer at 7 a.m. and at 7 p.m. a near-adiabatic (neutral) mixed layer up to a height of only 500 m capped by an isothermal layer. Based on these observations, two values of vertical temperature gradient, 0.005 Km^{-1} ("half adiabatic") and zero ("isothermal") were adopted for the analysis to bracket the range of uncertainty in atmospheric conditions.

The calculated and observed smoke cloud heights versus distance from the burn are shown in Figure 13. It is evident that the cloud rise was limited by the stable stratification of the atmosphere.

To estimate cloud width and depth, the graphs of σ_y and σ_z versus distance and Pasquill-Gifford stability category in Turner's [20] manual were used. Following the reasoning above with regard to stability, two Pasquill-Gifford "types" were assumed: D (neutral) and E (slightly stable). Since 95% of the mass of a Gaussian distribution lies within the interval -2σ to $+2\sigma$, $4\sigma_y$ was chosen to estimate the width and $4\sigma_z$ to estimate the vertical depth of the visible cloud. Figures 14 and 15 show these estimates for the distances at which "observed" values were obtained from the videotape for smoke plume width and depth respectively. As with the height estimate, the more stable case fits the smoke cloud characteristics best.

Smoke Concentration

Order of magnitude estimates of smoke mass concentration in the plume downwind of the burn were calculated consistent with the above analysis. Assuming a mass loss rate of 35-40 g/m^2s [12] and 8% of this in the form of smoke [7] the smoke emission rate from the 15 m diameter pool would be about 500 g/s. Using Turner's [20] graphs for σ_y and σ_z versus distance, with the Gaussian distribution model, we can estimate the plume centerline concentration

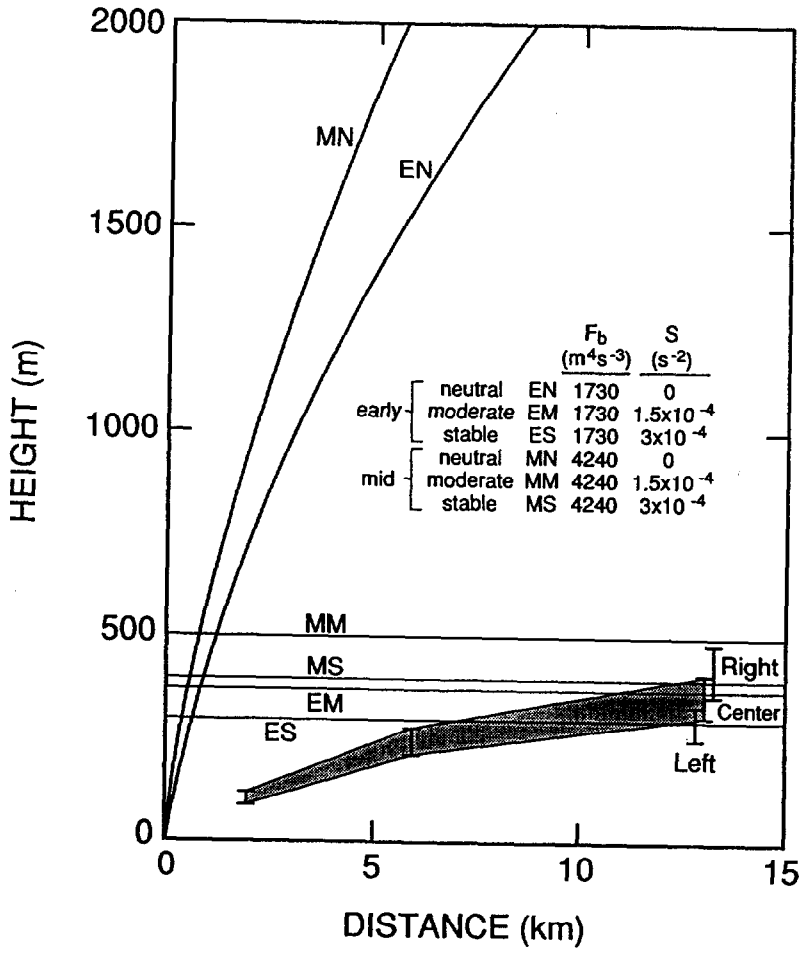

Figure 13 Smoke plume rise height versus distance from the burn.

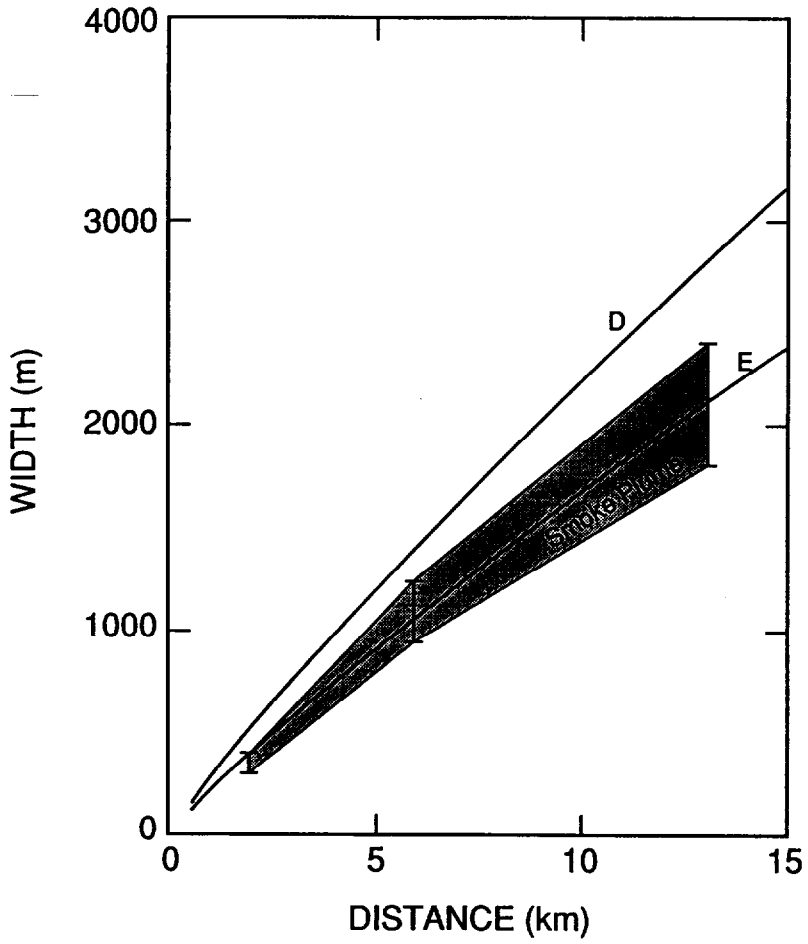

Figure 14 Smoke plume width versus distance from the burn.

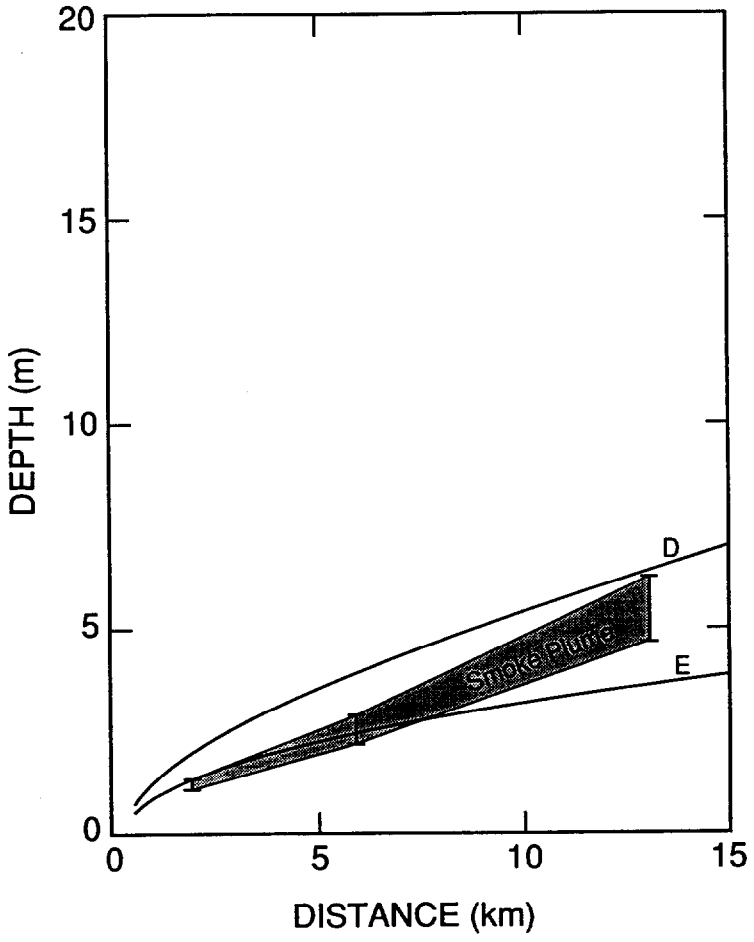

Figure 15 Smoke plume depth versus distance from the burn.

$$C(x,H) = Q/\pi\sigma_y\sigma_z u \quad (3)$$

and the ground-level concentration under the plume axis

$$C(x,O) = C(x,H) \exp(-H^2/2\sigma_z^2) \quad (4)$$

where

C (x,z) = concentration at distance x and height z,

Q = rate of emission, and

H = plume height

Calculated values for smoke mass concentration in the plume and in the air at ground level are shown in Figure 16 for Q = 500 g/s, H = 400 m and atmospheric stability type E (slightly stable).

For instrument package design, it is also necessary to know the nominal smoke mass concentration in the plume immediately downwind of the burning fuel. Using the same smoke emission rate as above (500 g/s) and a total speed of smoke flow in the plume of 3.5 m/s, from analysis of video data, the smoke concentration in the plume where the diameter is 30 m, (see Figure 12b), is 200 mg/m^3.

In view of the uncertainties and gaps in the available information it should be emphasized that the agreement or overlap between the ranges of observed and calculated parameters does not in itself confirm that the measurements, the assumed conditions, or the models are correct. Further analysis will be made of test records from future mid-scale tests in which more complete measurements particularly of atmospheric conditions will be made to determine the applicability of this model to smoke from crude oil burns.

These results are intended to illustrate the response of smoke transport to particular atmospheric conditions at the time and location of the burn at the Farrier Firefighting Facility at Norfolk, Virginia. Smoke plume dynamics are sensitive to local atmospheric conditions. For example, the temperature inversions typically occurring over Arctic ice surfaces would limit plume rise and vertical spread more severely, while the relatively vigorous convection over tropical waters would enhance buoyant rise and vertical mixing compared to the results obtained at Norfolk, Virginia.

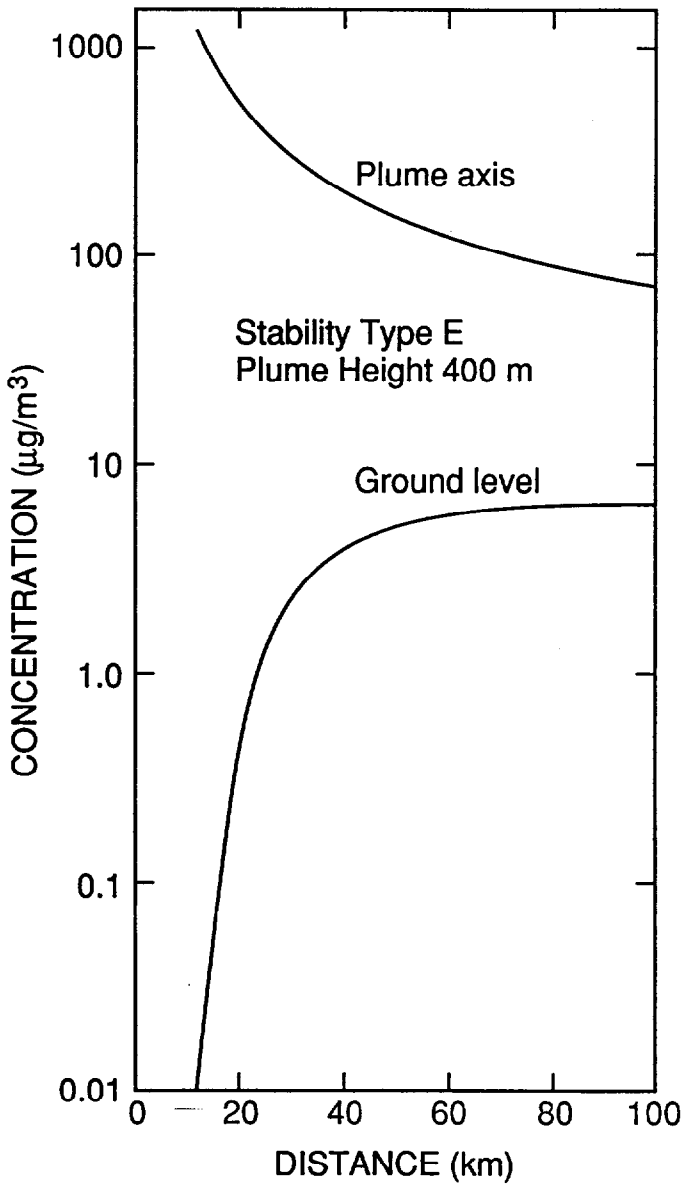

Figure 16 Calculated smoke concentration versus distance from the burn.

Vortex/Transport Element Method

The analysis in the previous section depends on information from experimental correlations of smoke dispersion from many studies. Another method to calculate smoke dispersion has become practical in recent years because of advances in computational methods and hardware. These methods make use of techniques to simulate numerically the turbulent mixing of smoke in the atmosphere.

The smoke plume model described in earlier paper from this research [8] has been implemented using a variant of the vortex element flow simulation technique developed by Ghoniem and his collaborators[21]. This technique, known as the transport element method [22, 23], has been applied to study the dynamics of turbulent shear layers, jets, and wakes. More recently, it has been extended to permit simulation of the Rayleigh-Taylor instability [24], a fundamental problem in gravity-driven flows. The code developed for this latter problem is the starting point for the calculations of the smoke plume settling displayed below. At the current stage of development, simulation capability is limited to consideration of the transport of a negatively buoyant plume of initially circular cross-section. The atmosphere is assumed to be unstratified, and the ambient wind is uniform. The research program currently under way will ultimately remove all of these restrictions.

Even at its current stage of development, the mathematical model exhibits many features of real turbulent mixing which are lost in models which assume prescribed forms for density and/or velocity profiles. These mechanisms are most readily explained by following the sequence of six frames from a simulation illustrated in Figures 17a-f. Each frame consists of a cross-sectional slice through the plume at successive stations downwind from the initial point. The uniform wind is coming out of the plane of the plots toward the viewer. Each curve represents a contour of constant particulate density as computed by the model. The innermost contour in the initial frame (Figure 17a) represents the maximum particulate density, which is then constant across the remainder of the interior. The outermost contour corresponds to zero particulate density. The ground is located at the bottom boundary of each plot. The numbers along the boundaries measure distance in units of the initial density gradient length, ℓ. This length specifies the initial particulate density profiles, ρ_P, as follows:

$$\rho_P - \rho_M \left[\frac{1 - \mathrm{erf}\left[\frac{r-\ell}{L} \right]}{2} \right] \qquad (5)$$

Here, ρ_M is the maximum particulate density, r is the radial coordinate measured from the center of the initial distribution, L is the nominal initial plume radius, and erf denotes the error function. The gradient length is physically significant in understanding the mixing process, as will be explained below.

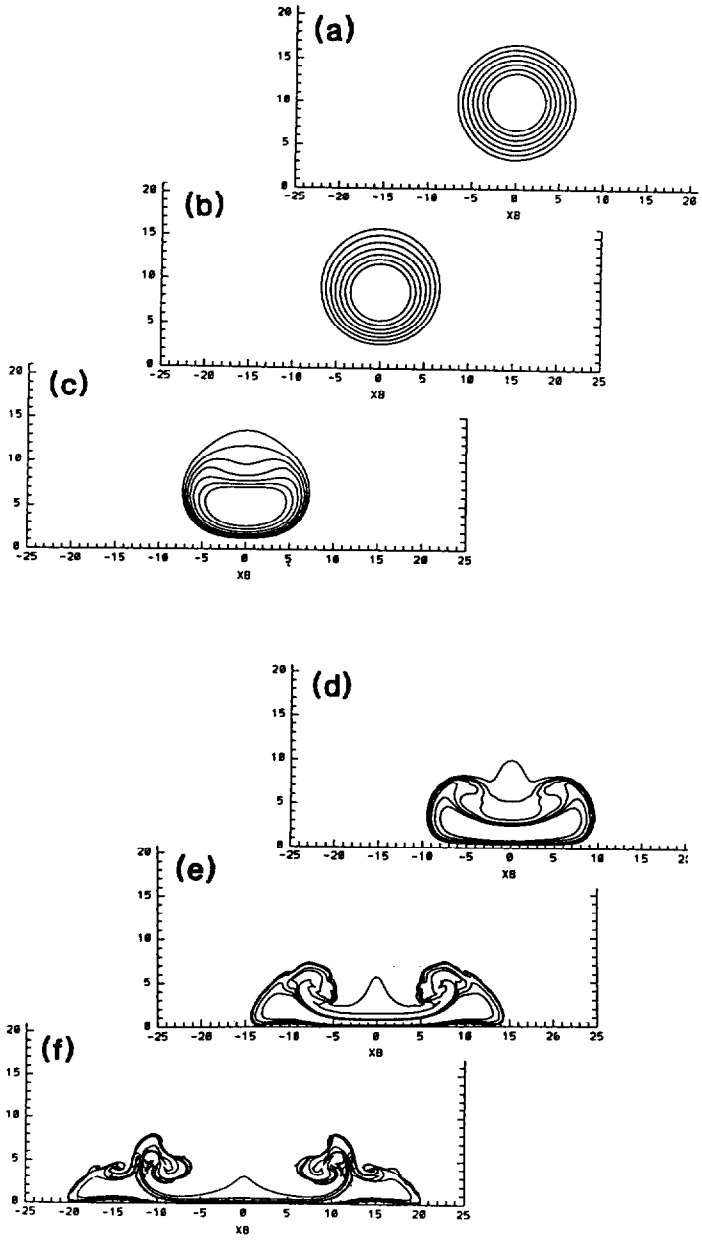

Figure 17 Plume vortex/transport element method output.

Now consider the sequence in detail. The first frame in Figure 17a shows the prescribed initial state of the plume, centered ten units above ground. Since horizontal density gradients induce vorticity fields opposite to the sign of the density gradient, positive vorticity is induced on the right side of the plume, and negative vorticity is induced on the left hand side. No vorticity is initially formed at the top or bottom of the plume. This pattern induces downward velocities everywhere in the plume, accompanied by the slight flattening seen in the second frame, Figure 17b. Note that the entire plume is displaced downward. The overall elliptical shape usually assumed in plume dispersion modeling is present for the first and only time in the simulation. The third frame, Figure 17c, shows the beginnings of the classical horseshoe shape widely observed in windblown plumes, modified by a flattening of the center portion caused by the presence of the ground.

The evolution is followed further in Figure 17d. This frame shows the further flattening of the plume as the opposite signed vorticity on each side of the plume interacts with the image vortices generated by the ground and are forced away from each other. This results in further distortion of the density contours, which generate strong secondary vorticity patterns. These secondary vortices act to entrain large amounts of clear air by sending out large tongues of particle laden air, engulfing volumes of surrounding atmosphere as shown in the fifth frame, Figure 17e. At each stage, the stretching and engulfing actions introduce smaller and smaller length scales into the problem. The horizontal density gradients become larger, inducing more intense vorticity, which further stretches and convolutes the density field, as shown in the final frame, Figure 17f. By this point in the simulation, the ratio of the maximum length scale, the overall geometric width, to the minimum gradient length, which generates the vorticity, is approaching 500.

These simulations which can be (and are) being performed on relatively modestly priced computer resources, permit the large scale turbulent mixing processes to be simulated directly without assuming anything about either the shapes of the velocity and density profiles, or the nature of the turbulence induced by the plume. When suitably extended to include more realistic scenarios and atmospheric phenomena, this methodology offers the promise of major improvements in predictive capability.

FUTURE RESEARCH

Many of the results reported here are ideas about how measurements and predictions will be made in both future mid-scale and field scale oil burn tests. During the following year, methods described here will be tested and evaluated in an extensive series of mid-scale test crude oil fires nominally 15 m in diameter. It is expected that these tests will identify needed improvements in the both the measurement and prediction methods being developed. Through this experience

improvements will be introduced into the hardware and software being developed in this research program, so that the best possible measurements can be obtained in the field scale burned planned for 1991.

ACKNOWLEDGEMENTS

This work was largely supported by the Minerals Management Service, U.S. Department of the Interior. Recognition is gives to Mr. Ed Tennyson and Mr. John Gregory who organized and consulted in the development of this research program. Special technical assistance and cooperation was provided by Dr. Merv Fingas of the Technology Development and Technical Services Branch, Environment Canada. Dr. George Mulholland of the Center for Fire Research, NIST provided considerable guidance to the project on methods of soot measurement. Dr. William Kelly of the Center for Analytical Chemistry, NIST provided expertise in techniques of particle measurement with isotopic tracers. Mr. Jay McElroy provided the engineering design and construction of the model to simulate oil burning within a boom. Mr. Nelson Bryner, Mr. Richard Zile, Mr. Roy McLane, and Mr. Gary Roadarmel provided technical support in the large laboratory fire tests. We are all grateful for the opportunity provided by the fire fighters and instructors at Navy's Farrier Firefighting Facility in Norfolk VA to observe and measure large fuel oil fires as preparation for the crude oil fire measurement program. This provided all researchers with insight that can not be gained in any other way.

REFERENCES

[1] Jason, N. J., editor, Alaska Arctic Offshore Oil Spill Response Technology - Workshop Proceedings, November 29-December 1, 1989, Anchorage, Alaska, NIST SP 762, U.S. Government Printing Office, Washington, DC, April 1989.

[2] USCG R&D Center, Groton Connecticut, Report of the Interagency Planning Workshop on Oil Spill Research and Development, September 26-27, 1989, Groton, Connecticut, Conference Report 90-30-1509.2, November 1989.

[3] U.S. Congress, Office of Technology Assessment, Coping with an Oiled Sea: An Analysis of Oil Spill Response Technology, OTA-BP-O-63, Washington, DC, U.S. Government Printing Office, March 1990.

[4] Allen, A., "Contained Controlled Burning of Spilled Oil During the Exxon Valdez Oil Spill," submitted to Thirteenth Arctic and Marine Oilspill Program Technical Seminar, June 6-8, 1990, Edmonton, Alberta.

[5] Evans, D., Baum, H., McCaffrey, B., Mulholland, G., Harkleroad, M., and Manders, W., "Combustion of Oil on Water," Proceedings of the Ninth Arctic Marine Oilspill Program Technical Seminar, June 10-12, 1986, Edmonton, Alberta, Ministry of Supply and Services Canada Cat. No. En 40-11/5-1986E, pp. 301-336, 1986.

[6] Evans, D., Mulholland, G., Gross, D., Baum, H., and Saito, K., "Environmental Effects of Oil Spill Combustion," Proceedings of the tenth Arctic and Marine Oilspill Program Technical Seminar, June 9-11, 1987, Edmonton, Alberta, Ministry of Supply and Services Canada Cat. No. En 40-11/5-1987E, pp. 91-130, 1987.

[7] Evans, D., Mulholland, G., Gross, D., Baum, H., and Saito, K., "Burning, Smoke Production, and Smoke Dispersion from Oil Spill Combustion," Proceedings of the Eleventh Arctic and Marine Oil Spill Program Technical Seminar, June 7-9, 1988, Vancouver, British Columbia, Ministry of Supply and Services Canada, Cat. No. En 49-11/5-1988 E/F, pp. 41-87, 1988.

[8] Evans, D., Baum, H., Mulholland, G., Bryner, N., and Forney, G., "Smoke Plumes From Crude Oil Burns," Proceedings of the Twelfth Arctic and Marine Oil Spill Program Technical Seminar, June 7-9, 1989, Calgary, Alberta, Ministry of Supply and Services Canada, Cat. No. En 40-11/5-1989, pp. 1-22, 1989.

[9] Parker, W.J., "Calculations of the Heat Release Rate by Oxygen Consumption for Various Applications," Journal of Fire Sciences, 2, pp. 380-395, 1984.

[10] Koseki, H., Mulholland, G., Tadahisa, J., "Joint Study on Liquid Pool Fire Between NIST/CFR and FRI - Part 1 Study on Combustion Property of Crude Oil," Tenth Joint Panel Meeting of the UJNR Panel on Fire Research and Safety, October 19-24, 1989, Berkeley, CA, (in press)

[11] Shokri, M. and Beyler, C.L. "Radiation From Large Pool Fires", J. of Fire Prot. Engr., 1(4), pp. 141-150, 1989.

[12] Mudan, K., and Croce, P. "Fire Hazard Calculations for Large Open Hydrocarbon Fires", SFPE Handbook of Fire Protection Engineering, ED. P. DiNenno et. al., National Fire Protection Association, Quincy MA, Section 2, Chapter 4, pp. 45-87, 1988.

[13] Koseki,H. and Yumoto, T., "Air Entrainment and Thermal Radiation from Heptane Pool Fires," Fire Technology, 24, pp. 33-47, 1988.

[14] Kelly, W. R. and Ondov, J. M., "Isotopic Tagging and Tracing of Pollutant Particles by Mass Spectrometry," Atmospheric Environment, in press.

[15] Mulholland, G. W., Henzel, V., and Babrauskas, V., "The Effect of Scale on Smoke Emission," Fire Safety Science--Proceedings of the Second International Symposium, pp. 347-357, 1989.

[16] King, T.Y., "Empirical Relationships Between Optical Density and Mass Density of Smoke," Journal of Fire and Flammability, 6, p. 222, 1975.

[17] Seader, J.D. and Ou, S.S., "Correlation of the Smoking Tendency of Materials," Fire Research, 1, pp. 3-9, 1977.

[18] Briggs, Gary A., "Plume Rise and Buoyancy Effects," Atmospheric Science and Power Production, U.S. Dept. of Energy, Washington, DC, pp. 327-366, 1984.

[19] List, Robert J., Smithsonian Meteorological Tables, Smithsonian Institution, Washington, DC, p. 527, 1958.

[20] Turner, D. Bruce, Workbook of Atmospheric Dispersion Estimates, U.S. Dept. of Health, Education and Welfare, Cincinnati, OH, p. 84, 1967.

[21] Ghoniem, A.F., Heidarinejad, G., and Krishnan, A., "Numerical Simulation of a Thermally Stratified Shear Layer Using the Vortex Element Method," J. Comp. Phys., 79, p. 135, 1988.

[22] Ghoniem, A.F., Heidarinejad, G., and Krishnan, A., "On Mixing, Baro-Clinicity, and the Effect of Strain in a Chemically Reacting Shear Layer," AIAA 26th Aerospace Science Meeting, Reno, AIAA-88-0729, 1988.

[23] Ghoniem, A.F., and Krishnan, A., "Origin and Manifestation of Flow-Combustion Interactions in a Premixed Shear Layer," Twenty Second Symposium (International) on Combustion, The Combustion Institute, Pittsburgh, p. 675, 1988.

[24] Krishnan, A. and Ghoniem, A.F., "Simulation of the Rollup and Mixing in Rayleigh-Taylor Flow Using the Vortex/Transport Element Method," J. Comp. Phys., in press.